Propagation of detached bubbles in a semi-infinite beam laid on a unilateral elastic support

Giovanni Lancioni
Dipartimento di Architettura, Costruzioni e Strutture, Università Politecnica delle Marche, Ancona, Italy. E-mail: g.lancioni@univpm.it

Keywords: wave propagation in beams, nonlinear non-smooth dynamics, absorbing boundary conditions in infinite beams.

SUMMARY. A moving-boundary problem governs the dynamics of a semi-infinite Bernoulli-Euler beam laid on a bed of unilateral elastic springs, being the positions of the touch-down points, those points which separate the detached beam parts from the laid ones, unknown. This problem is solved numerically by means of a self-made finite element code and some numerical results are shown. They point out the nonlinear and non-smooth effects of the touch-down points motion on the beam motion.

1 INTRODUCTION

This communication anticipates the main results of the paper [1], which improves and extends the study made in [2]. The nonlinear dynamics of a semi-infinite Bernoulli-Euler beam laid on a bed of unilateral elastic springs and subjected to an harmonic oscillation at the finite boundary and to a distributed downward load (see fig. 1 for a geometric scheme) is numerically investigated in [2] only in the case of a single touch-down point (TDP) which separates a detached part of the beam from the remaining semi-infinite laid part. We here study the dynamics when large oscillations imposed at the boundary produce the detachment of beam parts which, like bubbles, propagate through the beam. In the case of multiple TDPs, the resulting dynamics highlight much better the nonlinear and non-smooth features of the system due to the tensionless behavior of the supporting springs.

The studied problem constitutes a model for a lot of practical applications. As an example, in the field of civil engineering it schematizes pipes or foundations resting on soils, or, in the field of micromechanics, threads partially detached from an elastic support.

The beam dynamics is governed by a free-boundary problem, since the positions of the TDPs, which represent the boundaries between laid and detached parts of the beam, are unknown. In the case of a semi-infinite beam, an approximated analytical solution is determined in [3] by means of the asymptotic developments method, but only for motions characterized by a single TDP. If the analytical solution, evaluated up to the second order, is compared with the numerical solution (see [2]), good agreement is find between the analytical and numerical results only for small amplitudes of the excitation. When the forcing amplitude is increased, the effects of the problem nonlinearity on the motion became significant and the approximated analytical solutions result inaccurate. Moreover, the beam oscillations produce the detachment and propagation of beam parts which are not taken into account by the analytical solution. For a motion characterized by multiple TDPs, it is impossible to find exact solutions and the problem can only be handled numerically. To this end, a self-made Fem code has been developed. The discrete problem is reformulated in a finite domain by truncating the semi-infinite beam and by introducing first-order non-reflecting conditions on the artificial boundary. They are capable of perfectly filtering only a single prevailing harmonic progressive wave.

A systematic numerical investigation of the beam response is performed and the main effects of the problem nonlinearity on the dynamics, such as resonating superharmonic waves and bending

of the resonance peaks, are pointed out. Then, those motions characterized by more than one TDP are investigated, highlighting the effects of the non-smoothness. Complex behaviors like interrupted period doubling cascade and large period oscillations are observed.

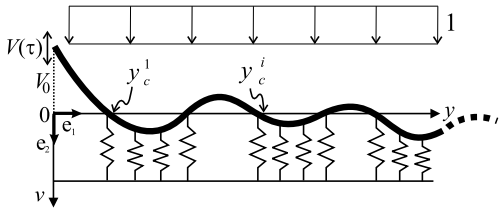

Figure 1: The problem geometry.

2 PROBLEM STATEMENT

We consider the semi-infinite beam depicted in Fig. 1, laid on a bed of unilateral elastic springs, loaded by a distributed downward force, and subjected to an harmonic vertical oscillation at the finite boundary. We assume the Bernoulli-Euler beam theory, so that the problem is governed by the dimensionless equations

$$\begin{array}{ll} \ddot{v} + \zeta\dot{v} + v'''' + v = 1, & \text{if } v \geq 0, \\ \ddot{v} + \zeta\dot{v} + v'''' = 1, & \text{if } v < 0, \end{array} \tag{1}$$

where $v = v(y, \tau)$ is the transversal displacement, witch depends on the dimensionless position y and time τ. A dot means a derivative with respect to τ and a prime a derivative with respect to y. Since the springs bed reacts only in compression, the reactive force per unit length v in (1) appears only when $v \geq 0$. The boundary conditions at $y = 0$ are

$$v(0, \tau) = V_0 + V\cos(\Omega\tau), \quad v''(0, \tau) = 0, \tag{2}$$

where V_0 is a fixed displacement and V and Ω are the amplitude and frequency of the imposed harmonic oscillation of period $T = 2\pi/\Omega$. The TDPs $y_c^i(\tau)$, $i = 1, ..., N$, satisfy the equations $v(y_c^i(\tau), \tau) = 0$. The semi-infinite length of the beam is taken into account by requiring that the motion must be bounded as y goes to infinite, and that incoming waves with finite amplitude are not allowed (radiation condition, see [4]). We refer to [1, 2] for the relations between the dimensionless quantities here considered and the usual dimensional ones.

2.1 *Analytical solutions*

If we suppose a single TDP y_c, approximated analytical solutions can be found by means of the asymptotic developments method. In [1, 2, 3], the solutions pair $(v(y, \tau),\ y_c(\tau))$ was found as power series of the imposed oscillation amplitude V (assumed as a smallness parameter). The following second order solution was found

$$\begin{aligned} v(y, \tau) &= v_0(y) + V^2 v_{02}(y) + V u_1(y) e^{-i\Omega\tau} + V^2 u_2(y) e^{-i2\Omega\tau}, \\ y(\tau) &= y_0 + V^2 y_{02} - \frac{2V}{y_0 + \sqrt{2}} u_1(y_0) e^{-i\Omega\tau} + V^2 y_2 e^{-i2\Omega\tau}, \end{aligned} \tag{3}$$

where the first two terms represent the static solution, the third term is the principal harmonic, the linear part of the solution, and the fourth term, the superharmonic wave with frequency 2Ω, represents the primary effects of the problem nonlinearity. We refer to [1] for the explicit expression of

the wave-shape functions u_1 and u_2. We expect that, if higher order terms are considered, superharmonic waves add in the solution, and, accordingly, the solution would assume the form

$$v(y,\tau) = \hat{v}_0(y) + \sum_{j=1}^{\infty} \hat{u}_j(y) e^{-ij\Omega\tau}. \tag{4}$$

3 NUMERICAL MODEL

If the oscillation amplitude V is large, then the motion is characterized by multiple TDPs. Detached parts of the beam propagate toward the right like travelling bubbles. In this case analytical solutions are unavailable and thus approximated numerical solutions are looked for.

To numerically handle the problem, a self-made code was developed. It combines the finite element method (in space) and the incremental Newmark method (in time), and consider the TDPs as movable extra nodes added to the mesh fixed nodes. Their unknown positions are determined by means of an iterative procedure within each time step.

Moreover, since the semi-infinite beam cannot be discretized by means of a limited number of finite elements, the problem is reformulated in a finite domain of length L by truncating the semi-infinite beam and by introducing first order non-reflecting conditions on the artificial boundary. These conditions are capable of totally absorbing only one outgoing harmonic progressive wave with a given frequency.

3.1 *First-order absorbing boundary conditions*

Let $y = L$ be a point quite distant from the finite boundary $y = 0$, and such that it never detaches from the springs bed. We suppose that it undergoes a periodic oscillation of period $2\pi/h\Omega$, which is approximate by the binomial expression

$$v(L,\tau) = \hat{v}_0(L) + \hat{u}_h(L) e^{-ih\Omega\tau}, \tag{5}$$

where the first term is the static position and the second term is the oscillation due to the prevailing harmonic among all the harmonic waves of the beam motion (4). To define a criterium of selection of the predominant oscillation, let us analyze the wave-shape $\hat{u}_h$ for small values of the viscosity ($\zeta << 1$)[1]. The wave in the semi-infinite laid part of the beam, which the point $y = L$ belongs to, assumes the approximate spatial shape (see [1] for the details)

$$\begin{aligned} &\hat{u}_h(y) \simeq e^{-\frac{\sqrt{2}}{2}\alpha y}\left(a_1 e^{i\frac{\sqrt{2}}{2}\alpha y} + a_2 e^{-i\frac{\sqrt{2}}{2}\alpha y}\right), && \text{if } h\Omega < 1, \\ &\hat{u}_h(y) \simeq a_1 e^{i\alpha y} + a_2 e^{-\alpha y}, && \text{if } h\Omega > 1, \end{aligned} \tag{6}$$

with $\alpha = \sqrt{|(h\Omega)^2 - 1|}$. In the subcritical regime ($h\Omega < 1$), the oscillation is the sum of two travelling waves, an outgoing wave and an incoming one, with amplitude exponentially decreasing in space. In the supercritical regime ($h\Omega > 1$), the motion is given by a travelling outgoing harmonic wave with constant amplitude and a standing wave with decreasing amplitude. It follows that at $y = L$ waves in the subcritical regime are negligible and the prevailing oscillation is due to the lowest supercritical harmonic, i.e., the h-th harmonic, with h the smallest integer such that $h < 1/\Omega$. Based on this consideration h is chosen as follows

$$\begin{aligned} &h = 1, \text{ if } 0 \le \Omega < 1/3 \text{ or } \Omega \ge 1; \\ &h = 2, \text{ if } 1/2 \le \Omega < 1; \quad h = 3, \text{ if } 1/3 \le \Omega < 1/2, \end{aligned} \tag{7}$$

[1] In this case the wave motion propagates through the beam without being significantly attenuated by the viscosity, and absorbing conditions are useful. For large values of ζ, the motion is damped quickly through the beam and at a certain distance from the finite boundary the beam can be supposed at rest. It follows that, in this case, absorption is not required.

where only the first two superharmonics are considered, and those of order higher than two are supposed to be negligible.

Now we can evaluate the rotation $\varphi = -v'$, the shear force $T = -v'''$ and the bending moment $M = -v''$ from (5), and organize them in the following kinematical and dynamical vectors

$$\mathbf{u} := \begin{bmatrix} v(L) \\ \varphi(L) \end{bmatrix} = \mathbf{C}(h\Omega)\mathbf{w} + \mathbf{u}_0, \quad \mathbf{f} := \begin{bmatrix} T(L) \\ M(L) \end{bmatrix} = \mathbf{D}(h\Omega)\mathbf{w} + \mathbf{f}_0, \tag{8}$$

where $\mathbf{w} = \begin{bmatrix} a_1 \\ a_2 \end{bmatrix} \hat{u}_h(L)e^{-ih\Omega\tau}$, $\mathbf{u}_0$ and $\mathbf{f}_0$ are the kinematical and dynamical vectors in the static configuration, and $\mathbf{C}$ and $\mathbf{D}$ are complex matrices (their component-wise representations are given in [1]). Combining the equations (8), we obtain

$$\mathbf{f} = \mathbf{H}(\mathbf{u} - \mathbf{u}_0) + \mathbf{f}_0, \tag{9}$$

where $\mathbf{H} = \mathbf{D}\mathbf{C}^{-1}$ is a complex matrix. If we approximate the static solution for $y >> 1$ by $\hat{v}_0(y) = 1$, and we use the relations $(\mathbf{u} - \mathbf{u}_0) = i\dot{\mathbf{u}}/(h\Omega)$, and $(\mathbf{u} - \mathbf{u}_0) = -\ddot{\mathbf{u}}/(h\Omega)^2$, equation (9) can be rewritten in the form

$$\mathbf{f} = \mathbf{L}\mathbf{u} + \frac{1}{h\Omega}\mathbf{M}\dot{\mathbf{u}} + \frac{1}{(h\Omega)^2}\mathbf{N}\ddot{\mathbf{u}} + \mathbf{p}, \tag{10}$$

where $\mathbf{L}$, $\mathbf{M}$ and $\mathbf{N}$ are given positive-defined matrices which depend only on $h\Omega$, and $\mathbf{p}$ is a $(h\Omega)$-dependent vector.

The condition (10) at $y = L$ is implemented in the numerical code. Since it perfectly filters only the prevailing h-th harmonic, it is said of order one. Not reported numerical tests show that the absorbing condition (10) is efficient in the case of excitations which are harmonic, as the cosine displacement imposed at $y = 0$. In the case of non harmonic excitations, the efficiency of the condition (10) reduces. In this case, indeed, the dispersive propagation of waves through the beam is characterized by a multi-frequency spectrum, and the condition (10) can filter only one frequency, and partially reflects all the others. Higher order boundary conditions are required, capable of absorbing a wide number of frequencies. These conditions have been developed for the wave equation in [5, 6] and applied to a finite element model in [7], but we are not aware of analogous studies for the beam equation.

4 NUMERICAL SIMULATIONS

Two sets of numerical simulations are performed, corresponding to two different values of the amplitude V of the imposed oscillation at $y = 0$. For the static displacement $V_0 = -15$, the values $V = 0.5$ and $V = 2$ are considered. In the first case, the beam oscillation is characterized by a single TDP and the numerical results are very close to the linear first order solution ((3) truncated at the first order). In the second case, the nonlinear effects become relevant on the beam dynamics and the motion remarkably deviates from the first order analytical approximation. Moreover, multiple TDPs enter the oscillation, and bubbles, beam detached parts, propagate through the beam, highlighting the non-smooth character of the dynamics. The values of the other problem parameters assumed in the numerical tests are: beam length $L = 50$, mesh size $h = 0.5$, time step $dt = T/30$ ($T = 2\pi/\Omega$), and damping coefficient $\zeta = 0.05$.

A parametric analysis is performed by considering Ω as the varying (controlling) parameter. In Fig. 2, the bifurcation diagram of the oscillation of the first TDP y_c is plotted as a function of Ω,

for $V = 0.5$, $V = 2$ and for the linear first-order case (dotted line). At each fixed value of Ω, in the bifurcation diagram we report the sequence of points $y_c(nT)$, $n = n_t, n_t + 1, n_t + 2, ..., n_f$ (remind that $T = 2\pi/\Omega$), where n_t and n_f are positive integers such that $n_t T$ is the transient time and $n_f T$ the final time of observation. We typically use $n_t = 100$ and $n_f = 400$. In Fig. 3, the amplification factor D versus Ω is drawn. The amplification factor is defined $D = Y_c/V$, where Y_c is the maximum amplitude of the oscillation y_c, and it is determined by computing the semi-distance between the two extreme points of the oscillation y_c.

In the case $V = 0.5$ the closeness between the numerical and the first-order analytical curves of Figs. 2 and 3 corroborates the efficiency of the numerical code, on one hand, and states that the linear analytical solution provides a good approximation of the motion for small values of V (such as $V = 0.5$), on the other hand. We notice that at $\Omega \simeq 0.68$, the TDP oscillation resonates (Fig. 3) and exhibits a phase shift (Fig. 2).

In the case $V = 2$, the bifurcation diagram of Fig. 2 and the amplification factor of Fig. 3 significantly deviate from the corresponding linear curves. For $\Omega > 0.95$, the curves qualitatively differ from the linear ones, because multiple TDPs enter the motion and new dynamical behaviors are observed. They are described in the following.

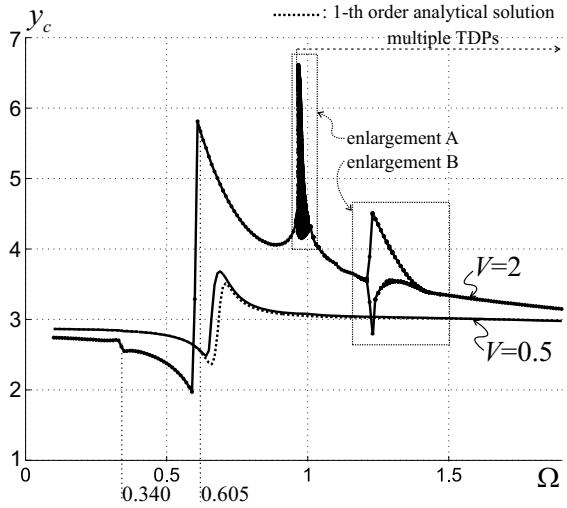

Figure 2: Bifurcation diagram of the first TDP oscillation y_c.

Principal and subcritical resonances

Looking at Fig. 3 we note that a subharmonic resonance appears at $\Omega \simeq 0.34$. Its frequency is half the linear resonance frequency ($\Omega \simeq 0.68$) and it is due to the amplification of the first superharmonic wave, with frequency 2Ω, which adds to the principal harmonic. The principal resonance curve increases its bending toward the left as an effect of the softening of the system [8], and reduces its maximum. Not-reported simulations show that for values of V bigger than 2, an hysteretic behavior takes place.

Let us analyze the oscillation y_c around the principal resonance. For $\Omega < 0.590$ it is essentially in counter phase with respect to the harmonic displacement applied at $y = 0$. A minimum value of $y_c = y_c(\tau)$ corresponds to a maximum of $v_o = v(0, \tau)$, and, on the contrary, a maximum of y_c

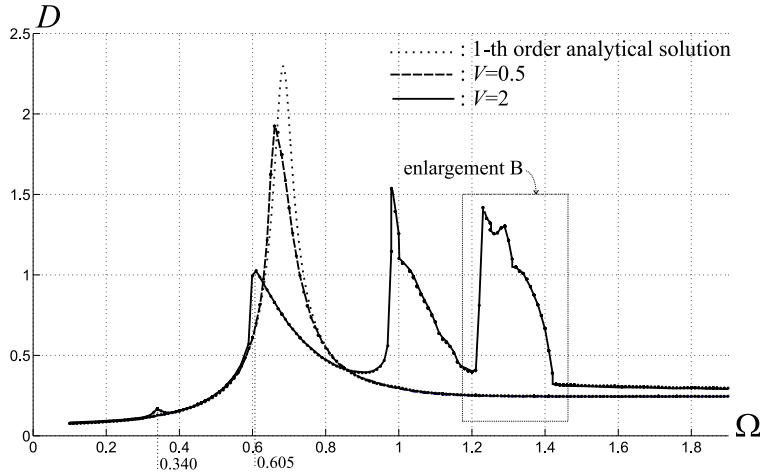

Figure 3: Amplification factor *D versus* Ω.

corresponds to a minimum of v_o. In the frequency range $0.590 < \Omega < 0.605$ the oscillation phase shifts of an angle of about π, and for $\Omega > 0.605$, y_c and v_o are in phase.

Multiple TDPs and motions of large period ($0.966 < \Omega < 1$**)**

In a neighborhood of $\Omega = 1$ an enlargement of the bifurcation diagram is reported in Fig. 4. For increasing values of Ω up to $\Omega = 0.975$, the motion is characterized by a single TDP, whose oscillation is of period T. In Fig. 5(a) the oscillation y_c is plotted for $\Omega = 0.972$, and its frequency spectrum is depicted Fig. 5(d). Peaks of superharmonic oscillations are an effect of the problem nonlinearity. This motion corresponds to the monotonically increasing bifurcation branch of Fig. 4. The branch slope increases up to become infinity at the point $\Omega = 0.975$, which looks like a saddle-node bifurcation point.

For $\Omega > 0.975$ multiple TDPs enter the motion. The trajectories followed by the TDPs are drawn in Fig. 5(b) for $\Omega = 0.978$. The gray-filled closed curves represent the propagating detached bubbles in the beam, highlighting the non-smooth character of the system. They define the position of the laid and detached parts of the beam at each time instant. In Fig. 5(c), as an example, the beam configuration at the instant $\tau = \bar{\tau}$ is depicted. It is characterized by a detached bubble, which propagates toward the right of the beam, as suggested by the TDPs trajectories. The oscillation y_c for $\Omega = 0.978$ (Fig. 5(b)) has period $19T$. The oscillation of period T is modulated by a period $19T$ wave. A kind of beating phenomenon takes place, which, perhaps, is due to the closeness between the forcing frequency and the critical frequency $\Omega = 1$. The frequency spectrum of such a motion is represented in Fig. 5(e), where it is compared with that for $\Omega = 0.972$. A peak appears at the frequency $\Omega/19$, corresponding to the modulating wave, and secondary peaks come up near the principal and superharmonic peaks, placed at a distance of $\Omega/19$ between each other. The period of the superposed wave reduces as Ω increases. Looking at the bifurcation diagram of Fig. 4, the motion in the frequency range $0.975 < \Omega < 1$ looks chaotic instead of periodic; however, in the frequency spectra (Figs. 5(e)) the broad band typical of chaotic signal is not so evident, so we conclude that it is a periodic oscillation with a small, minor, chaotic modulation.

The large period motion stops at $\Omega = 1$. For $\Omega \geq 1$ the period of y_c becomes again T, but multiple TDPs remain. At $\Omega = 1$ the transition from the large period motion to the period T

oscillation is very quick and is certainly influenced by the change in shape of the principal harmonic wave of the beam motion, which passes from the subcritical to the supercritical regime.

For decreasing values of Ω, the transition from a large period oscillation with multiple TDPs to a period T oscillation with a single TDP occurs at $\Omega = 0.966$ (Fig. 4), and an hysteretic behavior is observed.

Multiple TDPs and period doubling ($1.15 < \Omega < 1.45$**)**

In the frequency range $1.15 < \Omega < 1.45$, an enlargement of the bifurcation diagram and of the amplification coefficient curve is plotted in Fig. 6. Here, a (non smooth) period doubling bifurcation is observed in the oscillation of y_c, a phenomenon which is related to the appearance, evolution, and vanishing of bubbles. Motions of period one, two and four are found, and their frequency ranges are indicated in Fig. 6(a).

For $\Omega < 1.195$, the motion has period T. The TDPs trajectories are represented in Fig. 7(a), for $\Omega = 1.19$. The bubbles maintain their shape at each period. Since neighboring bubbles overlap in time, there are time intervals characterized by five TDPs, and two detached bubbles.

A period $2T$ oscillation starts at the bifurcation point $\Omega = 1.195$. The transition from period one to period two is related to the following bubbles evolution: at $\Omega = 1.195$ they begin to assume two different shapes which alternate in time, and, for increasing Ω, they take the forms shown in Fig. 7(b)-(c) for $\Omega = 1.21$ and $\Omega = 1.23$. Within a period $2T$, one bubble is attached to the trajectory y_c and the other one is separated from it and reduces in size. At $\Omega = 1.21$, the amplitude of the oscillation y_c attains a maximum (see Fig. 6(b)), and the bubbles propagate up to the point $y \simeq 23$, the most distant point reached by the TDPs.

At $\Omega = 1.245$ the oscillation y_c becomes of period $4T$ and the bifurcation branches double into two pairs. For increasing values of Ω the bubbles evolve as in Fig. 7(d)-(e). Within a period, first a bubble detached from the y_c trajectory (Fig. 7(d)), then a small fourth bubble appears (Fig. 7(e)). If Ω further increases, the bubbles attached to y_c separate from it, and, within a period, the four bubbles modify in order that the odd and the even bubbles assume two different shapes. The two pairs of bifurcation branches joint together into two curves at $\Omega = 1.295$ and the motion of y_c return to be again of period $2T$.

The frequency spectra of the oscillation y_c are plotted in Fig. 7(f)-(g)-(h) for $\Omega = 1.15$, $\Omega = 1.23$ and $\Omega = 1.26$, corresponding to motions of period T, $2T$ and $4T$, respectively. The subharmonic wave of frequency $\Omega/2$ is prevailing in Fig. 7 (g) and (h), but a subharmonic of frequency $\Omega/4$ appears in Fig. 7(h), according to the fact that here the period is $4T$.

For $1.295 < \Omega < 1.415$ the motion of y_c has period $2T$. When Ω increases, the bubbles modify so that they become one equal to the other. At $\Omega = 1.415$ they take the same shape and the motion of y_c becomes of period T.

5 CONCLUSIONS

The analysis of the system dynamics in the case of multiple TDPs highlights the non-smooth nature of the system. In particular, we note how the born and propagation of detached bubbles have strong effects in the supercritical regions. Multiple TDPs have been recognized to be at the root of both (i) large periodic, chaotically modulated, oscillations, and (ii) period doubling phenomena, which, contrarily to what usually occurs, do not evolve in a period doubling cascade.

Several developments can be sought and are worthy of further studies. In our opinion, however, the most important is that concerned with the development of a higher order non-reflecting boundary conditions, which will improve the adopted numerical scheme.

References

[1] Lancioni, G., Lenci, S., "Multiple Touch Down-Points and Non-smooth Nonlinear Dynamics of a Semi-infinite Beam on Unilateral Springs," send for publication.

[2] Lancioni, G., Lenci, S., "Forced nonlinear oscillations of a semi-infinite beam resting on unilateral elastic soil: analytical and numerical solutions," *J. of Computational and Nonlinear Dynamics*, **2**, 155-166, (2007).

[3] Demeio, L., Lenci, S., "Forced nonlinear oscillations of semi-infinite cables and beams resting on a unilateral elastic substrate," *Nonlinear Dynamics*, **49**, 203-215, (2007).

[4] Graff, K.F., "Wave motion in elastic solids," Oxford University Press, London, (1975).

[5] Engquist, B., Majda, A., "Absorbing boundary conditions for the numerical simulation of waves," *Mathematics of Computation*, Vol. **31**(139), 629-651, (1977).

[6] Higdon, R.L., "Radiation boundary conditions for dispersive waves," *SIAM J. Numer. Anal.*, **31**(1), 64-100, (1994).

[7] Givoli, D., Hagstrom, T., Patlashenko, I., "Finite element formulation with high-order absorbing boundary conditions for time-dependent waves," *Comput. Methods Appl. Mech. Engrg.*, **195**, 3666-3690, (2006).

[8] Nayfeh, A.H., Mook, D.T., "Nonlinear oscillations," Wiley Classics Library Edition Published, (1995).

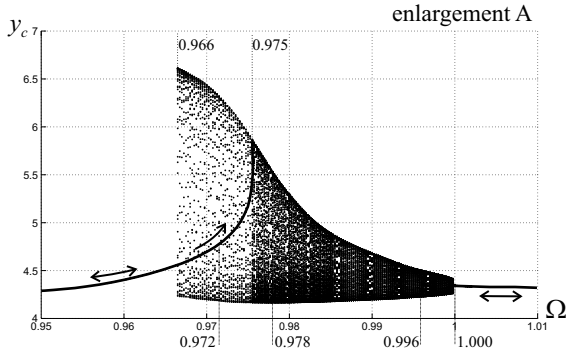

Figure 4: Bifurcation diagram in the frequency range $0.95 < \Omega < 1.01$.

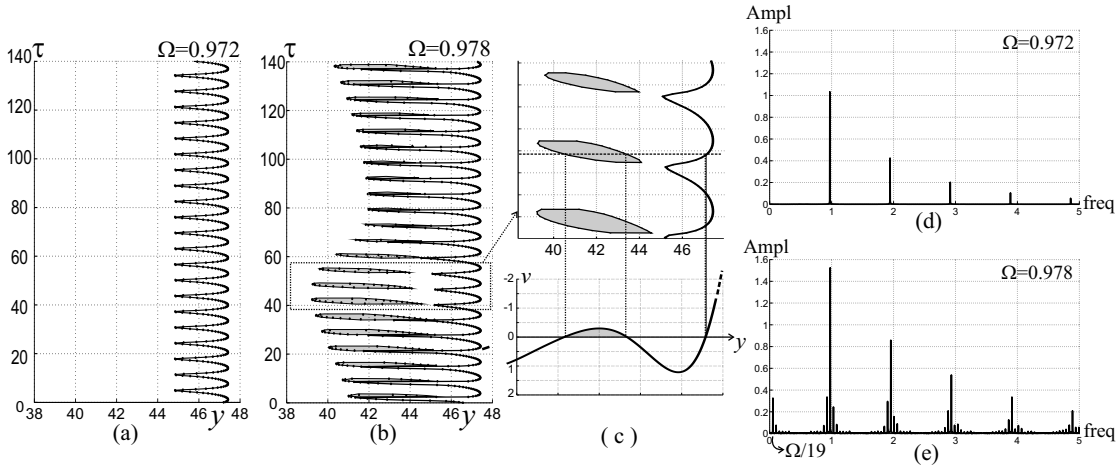

Figure 5: Time histories of the TDPs oscillations: (a) $\Omega = 0.972$ (single TDP); (b) $\Omega = 0.978$ (multiple TDPs); (c) enlargement of (b) and beam configuration at the time instant $\bar{\tau}$. Frequency spectra of y_c: (a) $\Omega = 0.972$; (b) $\Omega = 0.978$.

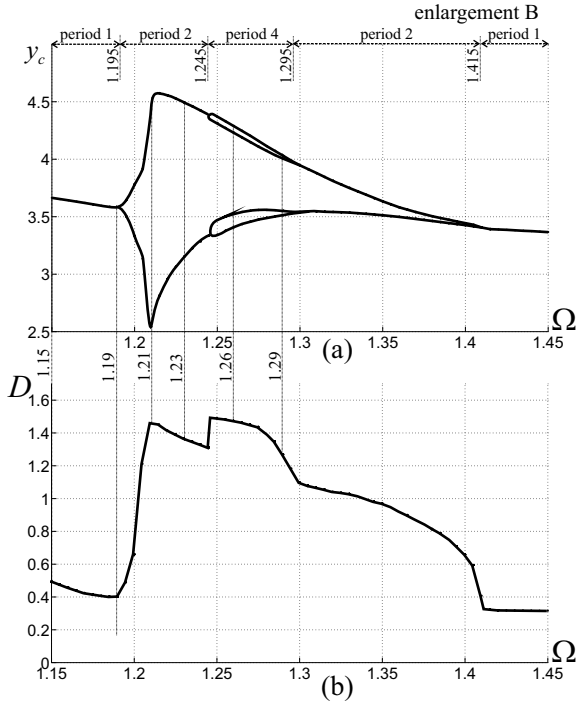

Figure 6: Bifurcation diagram (a), and coefficient of amplification D (b) in the frequency range $1.15 < \Omega < 1.45$.

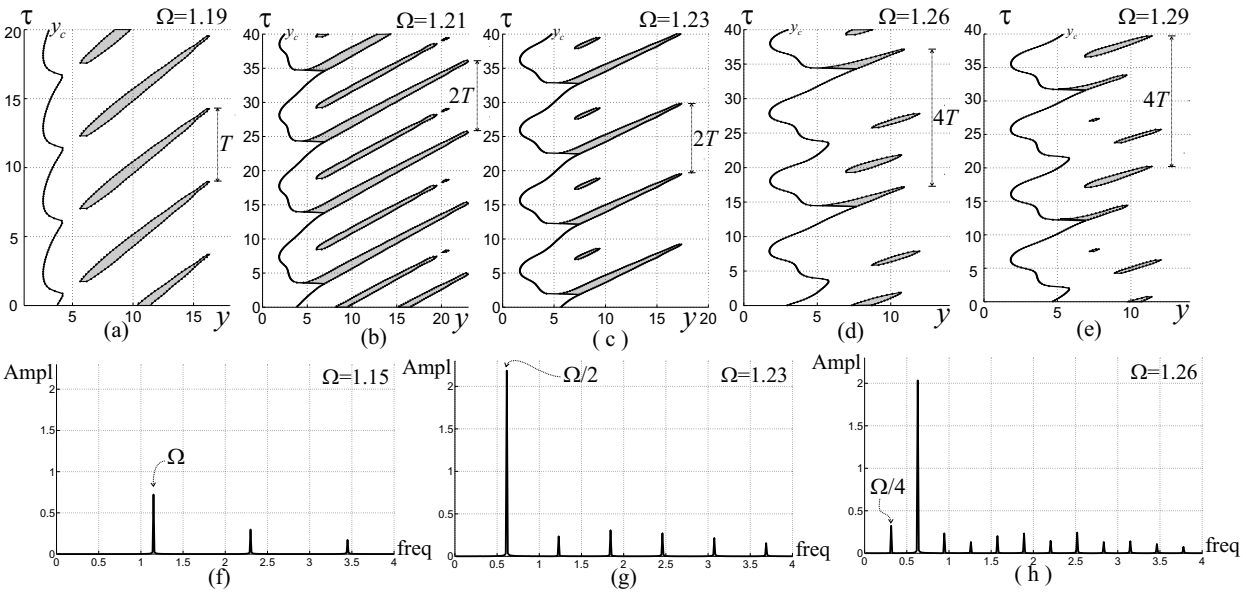

Figure 7: Time histories of the TDPs oscillations: (a) motion of period T; (b)-(c) motion of period $2T$; (d)-(e) motion of period $4T$. Frequency spectra of y_c: (f) $\Omega = 1.15$ (period one); (g) $\Omega = 1.23$ (period two); (h) $\Omega = 1.26$ (period four).